# Assessment of Seismic Design Provisions for Floor Diaphragms per ASCE/SEI 7-22

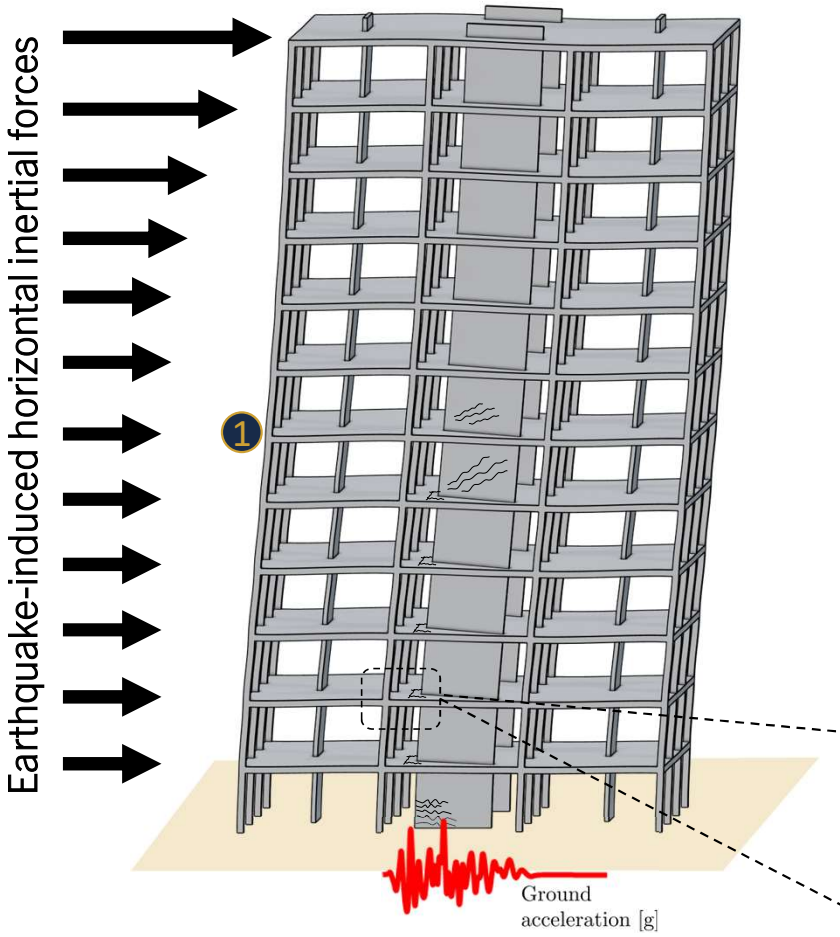
C. Franco Mayorga[1], Georgios Tsampras[2]

[1]Graduate Student Researcher, University of California San Diego, USA
[2]Assistant Professor, University of California San Diego, USA

July 5th, 2024

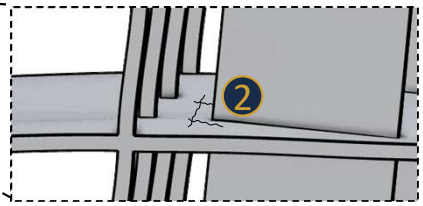
https://tsampras.ucsd.edu/

# Motivation: Floor Diaphragms and their Connections




Core wall building construction at UC San Diego






① Higher-mode responses
② Kinematic compatibility

Figures courtesy of Prof. Tsampras

# Motivation: Floor Diaphragm Seismic Responses and Failures in Past Earthquakes

[1]



**Fig. 2.** Precast parking structure collapse 1994 Northridge earthquake (photograph courtesy of Lacy Atkins, © 1994, Los Angeles Times; reprinted with permission)

[2]

*Lack of load path and adequate connection between diaphragm and wall:*

In several buildings, the lack of damage to some RC walls despite the apparent deformation demand on the remainder of the buildings suggests that the load path from, and connection to the floor diaphragm to the walls was poor and limited.

The 8-storey RC wall building shown in Figure 17 is an example of this. While four of the L-shaped RC walls in the East-West direction were damaged, the internal RC walls (also spanning in the East-West direction) shows a limited level of distress. The presence of voids (from services, lift and staircase penetrations) and limited diaphragm ties into the walls means limited inertia forces were transferred into these walls, despite being 'stiffer' than the L-shaped walls.

[3]



**Figure 5-1** Aerial view of collapsed roof in tilt-up-wall building.

**PERFORMANCE OF TILT-UP-WALL BUILDINGS**

The Northridge earthquake caused significant damage to tilt-up-wall buildings: the City of Los Angeles estimates that of the 1,200 tilt-up buildings in the San Fernando Valley, over 400 had significant structural damage (SSC 1994a), including partial roof collapse and collapse of exterior walls (Figure 5-1). Heavily damaged areas included Northridge, Chatsworth, Sylmar, and Sherman Oaks close to the epicentral area, but there was also significant damage in Newhall and Valencia to the north and in Santa Monica to the south.

[4]



*Fig. 2-9: Collapse of precast concrete hollow core floor (1994 Northridge earthquake)*



*Fig. 2-10: Flexible connections connecting diaphragm to precast concrete beam (1999 Kocaeli earthquake)*

[5]

Floor diaphragms play several roles in the seismic response of dual systems: support vertically spanning components, transfer lateral forces to walls and frames, provide restraint to columns and walls, tie the structure together, and enable redundant load paths for lateral forces. In many buildings after events as recent as the 2010-2011 Christchurch earthquakes, floor diaphragms were unable to perform one or more of these functions, leading to extensive damage and collapse. Research consistently highlights three underlying causes: a failure to ensure the integrity of the load path, underestimation of in-plane forces, and poorly understood interactions with walls, supporting beams and RC moment frames. Most recent and ongoing research has focused on modifying

[6]

Over 60% of the fatalities in the Christchurch earthquake on 22 February 2011 were due to the collapse of one modern building – the CTV Building. A major contributory factor to the collapse was the woefully deficient floor diaphragms. The building was almost completely dependent on the shear walls of the North Lift Core for its strength and stability, but there was no effective connection of the floors to that core.

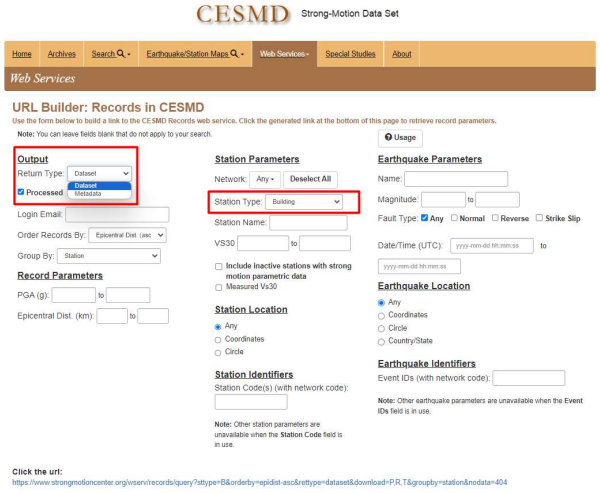
[7]

- The need to amplify lateral forces in diaphragms is understood. These actions arise from higher mode effects and the overstrength of a structure that is inherent and developed during inelastic response. A number of researchers and texts (NZCS, 1994, Paulay, 1996, Bull, 1997, Nakaki, 2000, Fleischman *et al*, 2001, Rodriguez *et al*, 2002) have suggested allowance for this overstrength feature.

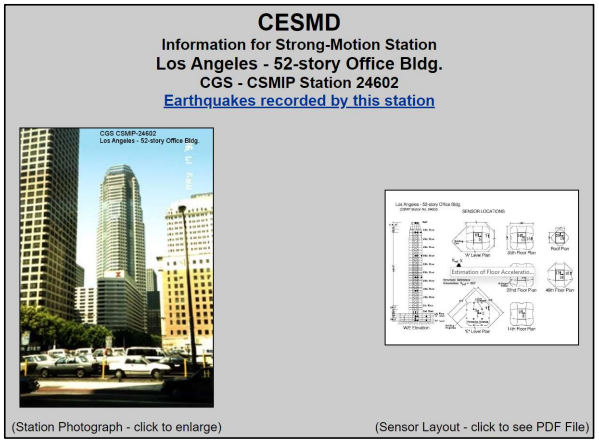

1. Fleischman, R. B., J. I. Restrepo, C. J. Naito, R. Sause, D. Zhang, and M. Schoettler. "Integrated Analytical and Experimental Research to Develop a New Seismic Design Methodology for Precast Concrete Diaphragms." Journal of Structural Engineering 139, no. 7 (July 2013): 1192–1204. https://doi.org/10.1061/(ASCE)ST.1943-541X.0000734.
2. Kam, W. Y., S. Pampanin, and K. Elwood. "Seismic Performance of Reinforced Concrete Buildings in the 22 February Christchurch (Lyttleton) Earthquake," 2011. https://ir.canterbury.ac.nz/handle/10092/9006.
3. "Tilt-up-Wall Buildings." Earthquake Spectra 12, no. 1_suppl (January 1, 1996): 99–123. https://doi.org/10.1193/1.1585922.
4. International Federation for Structural Concrete, ed. Seismic Design of Precast Concrete Building Structures: State-of-Art Report. Bulletin / International Federation for Structural Concrete 27. Lausanne: International Federation for Structural Concrete, 2003.
5. Gonzalez, A., E. Spacone, and R. Nascimbene. "Performance-Based Seismic Design Framework for RC Floor Diaphragms in Dual Systems." Procedia Engineering, X International Conference on Structural Dynamics, EURODYN 2017, 199 (January 1, 2017): 3546–51. https://doi.org/10.1016/j.proeng.2017.09.512.
6. Scarry, J M. "Floor Diaphragms – Seismic Bulwark or Achilles' Heel." In NZSEE Conference, 2014.
7. Bull, D. K. "Understanding the Complexities of Designing Diaphragms in Buildings for Earthquakes." Bulletin of the New Zealand Society for Earthquake Engineering 37, no. 2 (June 30, 2004): 70–88. https://doi.org/10.5459/bnzsee.37.2.70-88.

# Research Question

Can we utilize strong-motion data from actively monitored instrumented buildings to assess the seismic design provisions for floor diaphragms per ASCE/SEI 7-22, and how these provisions consider the higher-mode responses?




https://www.strongmotioncenter.org/wserv/records/builder/





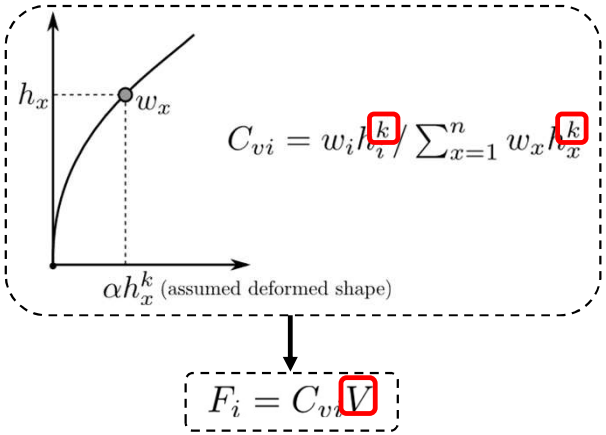



# ASCE/SEI 7-22[1] Seismic Design Provisions for Floor Diaphragms

Earthquake-induced horizontal floor diaphragm design force $F_{px}$ at floor level $x$.

- Section 12.10.1

$$F_{px} = \frac{\sum_{i=x}^{n} F_i}{\sum_{i=x}^{n} w_i} w_{px} \geq 0.2 S_{DS} I_e w_{px}$$




- Section 12.10.3 (alternative provisions)

$$F_{px} = \frac{C_{px}}{R_s} w_{px} \geq 0.2 S_{DS} I_e w_{px}$$

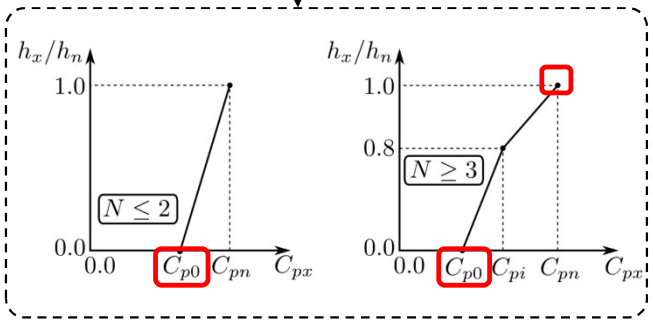
$$C_{pn} = \sqrt{(\Gamma_{m1} \Omega_0 C_s)^2 + (\Gamma_{m2} C_{s2})^2} \geq C_{pi}$$

$$C_{pi} = \max(0.8 C_{p0}, 0.9 \Gamma_{m1} \Omega_0 C_s)$$

$$C_{p0} = 0.4 S_{DS} I_e$$

$$\Gamma_{m1} = 1 + z_s(1 - 1/N)/2$$

$$\Gamma_{m2} = 0.9 z_s (1 - 1/N)^2$$




1. ASCE/SEI 7-22 (2021). Minimum design loads and associated criteria for buildings and other structures. American Society of Civil Engineers. https://doi.org/10.1061/9780784415788.



# ASCE/SEI 7-22[1] Seismic Design Provisions for Floor Diaphragms

Earthquake-induced horizontal floor diaphragm design force $F_{px}$ at floor level $x$.

- Section 12.10.1

$$F_{px} = \frac{\sum_{i=x}^{n} F_i}{\sum_{i=x}^{n} w_i} w_{px} \geq 0.2 S_{DS} I_e w_{px}$$

- Section 12.10.3 (alternative provisions)

$$F_{px} = \frac{C_{px}}{R_s} w_{px} \geq 0.2 S_{DS} I_e w_{px}$$

Floor diaphragm design acceleration coefficients at floor level $x$:

- Section 12.10.1

$$C_{px}^{(1)} = F_{px}/w_{px}$$

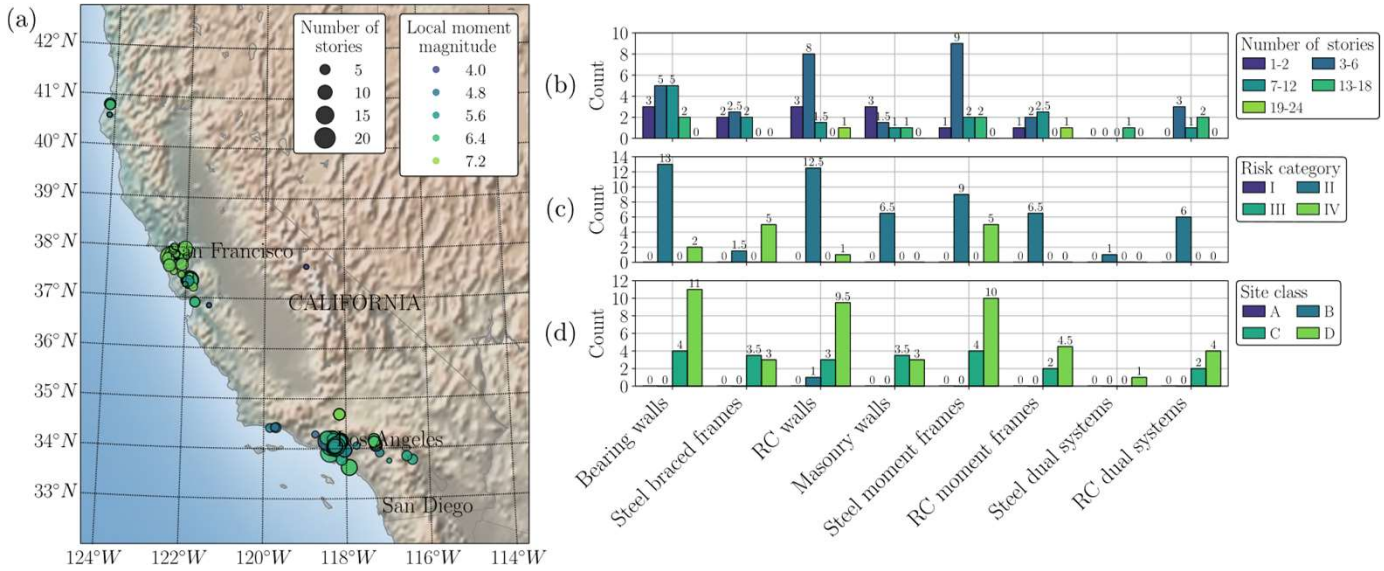
- Section 12.10.3

$$C_{px}^{(3)} = C_{px}$$

1. ASCE/SEI 7-22 (2021). Minimum design loads and associated criteria for buildings and other structures. American Society of Civil Engineers. https://doi.org/10.1061/9780784415788.

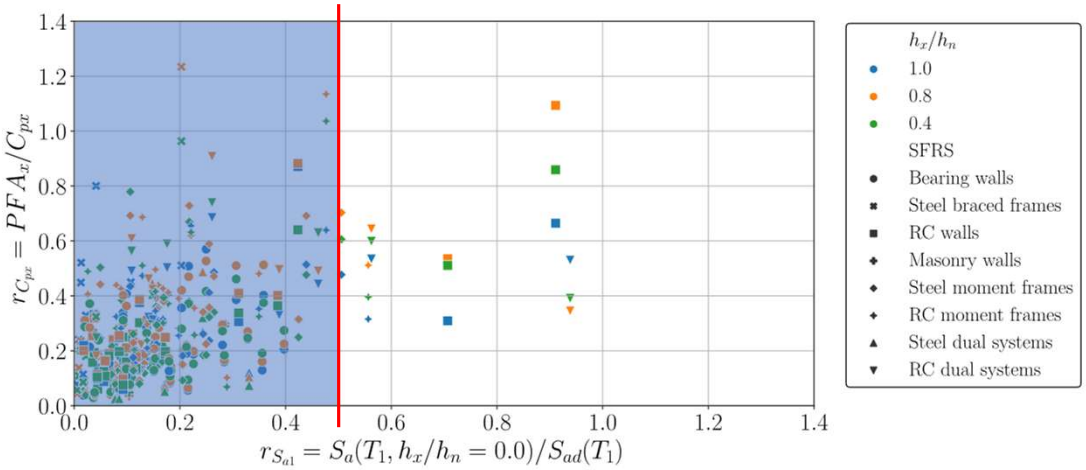
# Studied Building Stations

- 69 of the building stations monitored by the California Strong-Motion Instrumentation Program (CSMIP).
- More than 100 combinations of building stations and measured seismic events.



# Challenges

1. A lack of measured ground motions resulting in spectral accelerations close to the design earthquake intensity level.

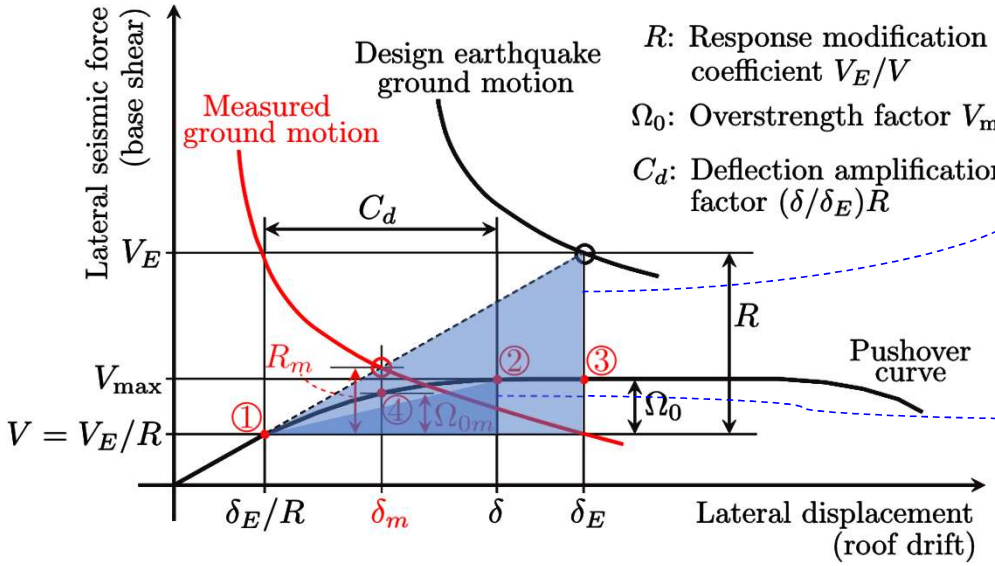



- $C_{px}^{(1)}$ and $C_{px}^{(3)}$ need to be scaled to the intensity level of the measured ground motions.

2. The inelastic response of the building stations subjected to the measured ground motions is limited.
   - $R$ and $\Omega_0$ need to be adjusted accordantly.

# Estimates of Seismic Performance Factors[1]

- Simplified and practical way to estimate $R$ and $\Omega_0$.
- This approach assumes that $\delta \approx \Delta_a$ and a linear variation of $\Omega_{0m}$ in terms of $\delta_m$.




$$R_m = \begin{cases} 1.0 & \text{if } \delta_m < \dfrac{\delta_E}{R} = \dfrac{\Delta_a}{C_d} \\ 1.0 + \dfrac{R - 1.0}{\dfrac{\Delta_a}{C_d}(R - 1.0)}\left(\delta_m - \dfrac{\Delta_a}{C_d}\right) & \text{if } \dfrac{\Delta_a}{C_d} \le \delta_m < \dfrac{\Delta_a}{C_d}R \\ R & \text{if } \delta_m \ge \delta_E = \dfrac{\Delta_a}{C_d}R \end{cases}$$

$$\Omega_{0m} = \begin{cases} 1.0 & \text{if } \delta_m < \dfrac{\delta_E}{R} = \dfrac{\Delta_a}{C_d} \\ 1.0 + \dfrac{\Omega_0 - 1.0}{\dfrac{\Delta_a}{C_d}(C_d - 1.0)}\left(\delta_m - \dfrac{\Delta_a}{C_d}\right) & \text{if } \dfrac{\Delta_a}{C_d} \le \delta_m < \Delta_a \\ \Omega_0 & \text{if } \delta_m \ge \Delta_a \end{cases}$$

$\delta$: Roof drift of the SFRS corresponding to the design-level earthquake assuming that the system has reached the plastic range.

$\delta_E/R$: Roof drift of the SFRS corresponding to $V$.
$\delta_E$: Roof drift of the SFRS corresponding to $V_E$.

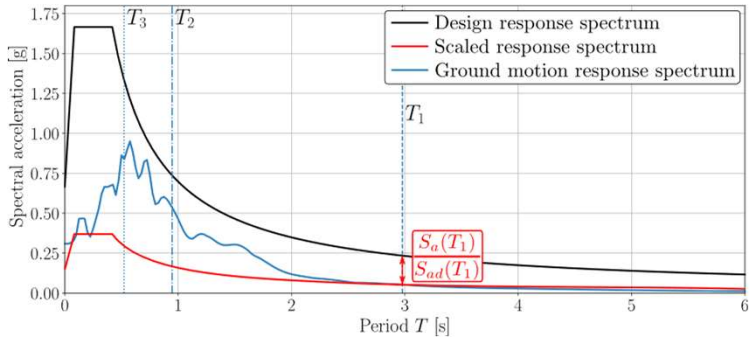
$\delta_m$: Measured roof drift.
$\Delta_a$: Allowable roof drift per ASCE 7-22 Table 12.12-1 for $h_{sx} = h_n$.

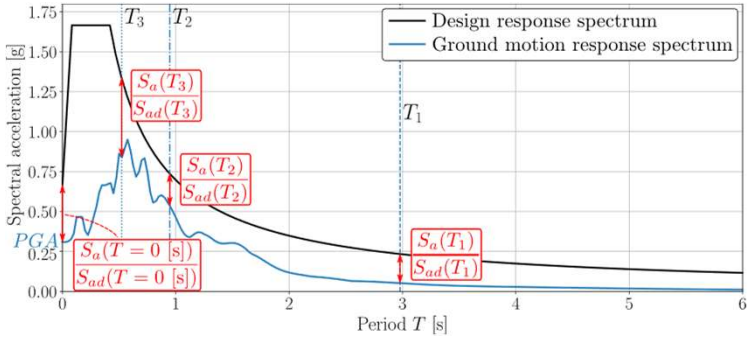

1. Federal Emergency Management Agency (FEMA) (2009). FEMA P695 Recommended Methodology for Quantification of Building System Performance and Response Parameters. Project ATC-63, Prepared by the Applied Technology Council, Redwood City.

# Design-based Intensity-dependent Acceleration Coefficients $C_{px,m}^{(j)}$

Six modification approaches ($m = 1, \dots, 6$) are considered to compute $C_{px,m}^{(j)}, j = 1,3$.

- Approach 1
  - $R$ and $\Omega_0$ per ASCE/SEI 7-22.
  - $C_{px,1}^{(j)} = C_{px}^{(j)}, j = 1,3$ scaled by $r_{S_{a1}} = S_a(T_1)/S_{ad}(T_1)$.
- Approach 2
  - $R = 1.0$ and $\Omega_0 = 1.0$.
  - $C_{px,2}^{(j)} = C_{px}^{(j)}, j = 1,3$ scaled by $r_{S_{a1}} = S_a(T_1)/S_{ad}(T_1)$.
- Approach 3
  - $R = R_m$ and $\Omega_0 = \Omega_{0m}$.
  - $C_{px,3}^{(j)} = C_{px}^{(j)}, j = 1,3$ scaled by $r_{S_{a1}} = S_a(T_1)/S_{ad}(T_1)$.
- Approach 4
  - $R = R_m$ and $\Omega_0 = \Omega_{0m}$.
  - $C_{px,4}^{(3)} = C_{px}^{(3)}$ scaled by $r_{S_{a12}} = \frac{\sqrt{S_a(T_1)^2 + S_a(T_2)^2}}{\sqrt{S_{ad}(T_1)^2 + S_{ad}(T_2)^2}}$.
- Approach 5
  - $R = R_m$ and $\Omega_0 = \Omega_{0m}$.
  - $C_{px,5}^{(3)} = C_{px}^{(3)}$ scaled by $r_{S_{a123}} = \frac{\sqrt{S_a(T_1)^2 + S_a(T_2)^2 + S_a(T_3)^2}}{\sqrt{S_{ad}(T_1)^2 + S_{ad}(T_2)^2 + S_{ad}(T_3)^2}}$.
- Approach 6
  - $R = R_m$ and $\Omega_0 = \Omega_{0m}$.
  - $C_{px,6}^{(1)} = C_{px}^{(1)}$ computed considering $C_s = S_a(T_1)/R_m$.
  - $C_{px,6}^{(3)} = C_{px}^{(3)}$ computed considering
    $C_{p0} = S_a(T = 0[s]) = \text{PGA}$.
    $C_s = S_a(T_1)/R_m$.
    $C_{s2} = \max(S_a(T_2), S_a(T_3))$.



# $C_{px,m}^{(j)}$-to-$PFA_x$ Comparison Metrics

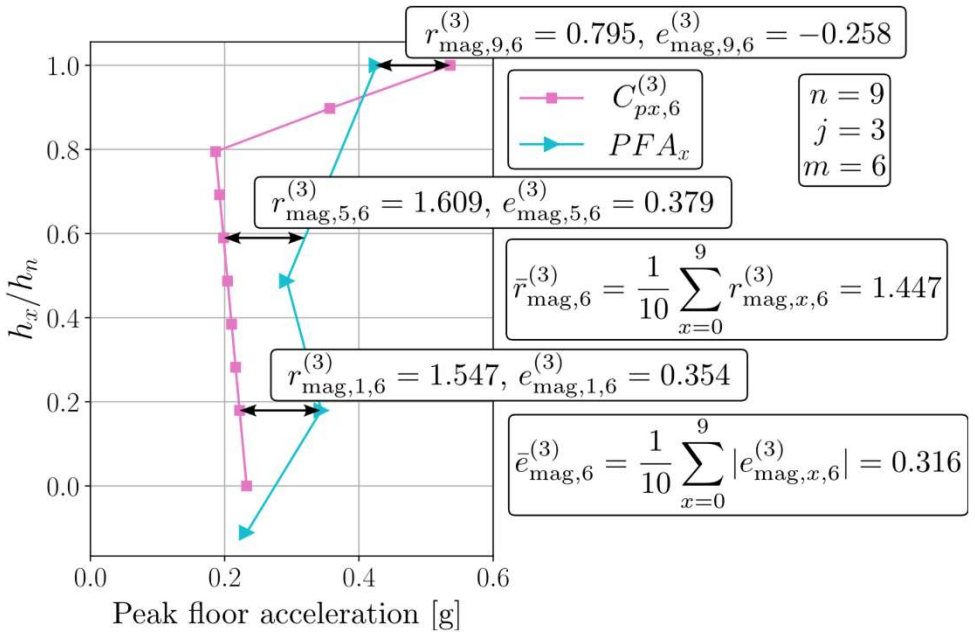
$PFA_x$ is compared with $C_{px,m}^{(j)}$, $j = 1,3$ and $m = 1, \ldots, 6$ over the height of the building stations.

$$\bar{r}_{\text{mag},m}^{(j)} = \frac{1}{n+1}\sum_{x=0}^{n} r_{\text{mag},x,m}^{(j)}$$

$$\bar{e}_{\text{mag},m}^{(j)} = \frac{1}{n+1}\sum_{x=0}^{n} |e_{\text{mag},x,m}^{(j)}|$$

where

$$r_{\text{mag},x,m}^{(j)} = \frac{PFA_x}{C_{px,m}^{(j)}} \qquad e_{\text{mag},x,m}^{(j)} = \frac{C_{px,m}^{(j)} - PFA_x}{PFA_x}$$



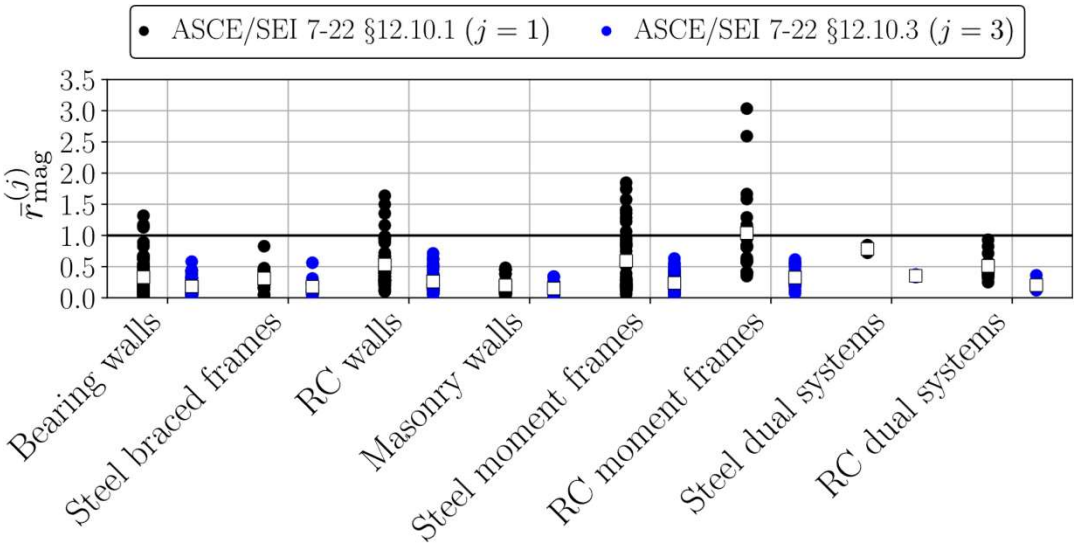
# Results: $C_{px}^{(j)}$-to-$PFA_x$ Comparison Metrics

The $c_{px}^{(1)}$ per ASCE/SEI 7-22 Section 12.10.1 underestimates the magnitude of the $PFA_x$ measured by many building stations subjected to ground motions with intensities lower than the design level.

$$\bar{r}_{\text{mag}}^{(j)} = \frac{1}{n+1} \sum_{x=0}^{n} r_{\text{mag},x}^{(j)}$$

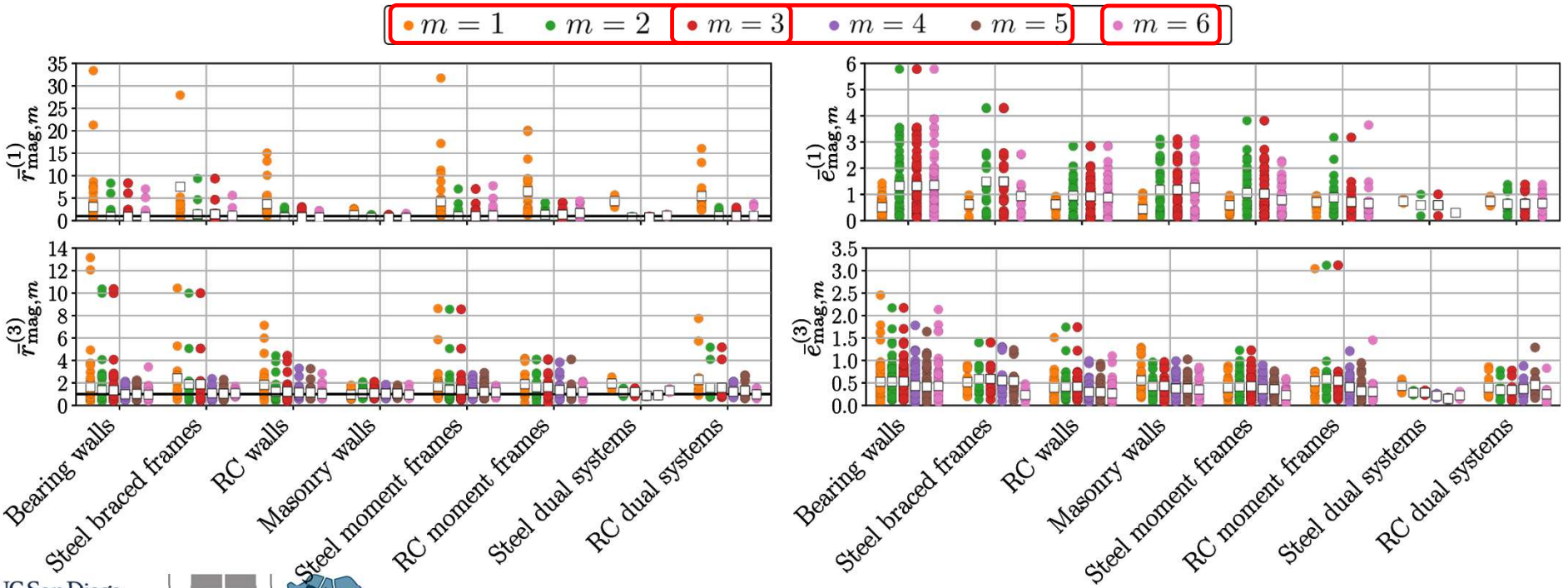
where

$$r_{\text{mag},x}^{(j)} = \frac{PFA_x}{C_{px}^{(j)}}$$



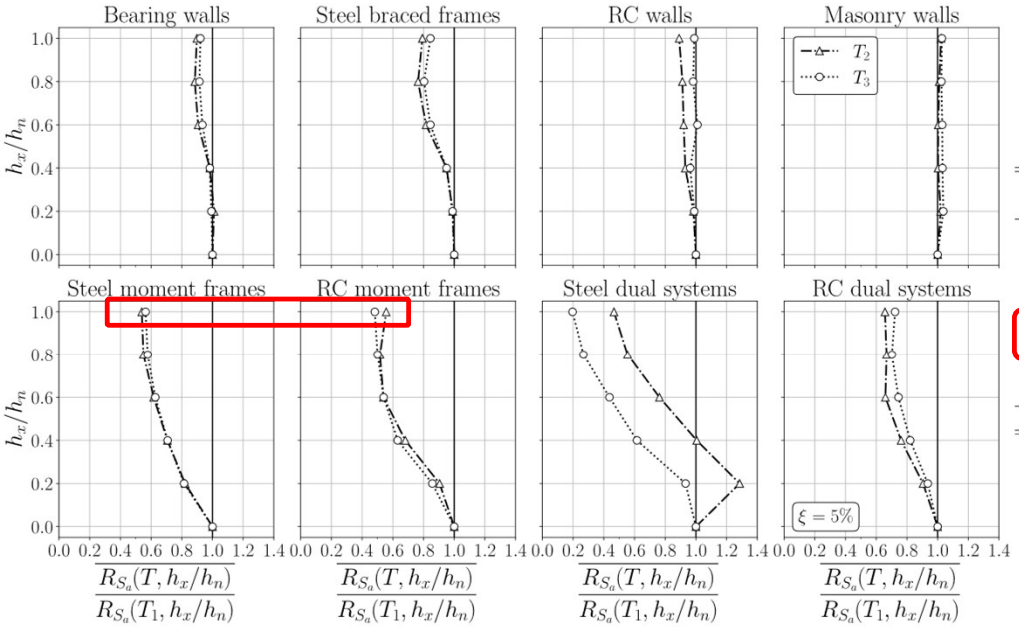
# Results: $C_{px,m}^{(j)}$-to-$PFA_x$ Comparison Metrics

- Considering $R_m$ and $\Omega_{0m}$ to modify the $c_{px}^{(1)}$ and $c_{px}^{(3)}$ improves the estimation of $PFA_x$.
- Considering $S_a(T_2)$ and $S_a(T_3)$ to scale the $c_{px}^{(3)}$ improves the estimation of $PFA_x$.
- The $c_{px,6}^{(3)}$ $(m = 6)$ better estimates the magnitude of the $PFA_x$.



# Results: Assessment of Higher-Mode Response

The mean values of the ratios of $R_{S_a}(T_i, h_x/h_n)$ for $i = 2, 3$ to $R_{S_a}(T_1, h_x/h_n)$ per seismic force-resisting system are investigated.




| SFRS | Count | Mean value $\mu$ (coefficient of variation $\sigma/\mu$ [%]) | |
|---|---|---|---|
| | | $R_{S_a}(T_2, h_x/h_n = 1.0)/R_{S_a}(T_1, h_x/h_n = 1.0)$ | $R_{S_a}(T_3, h_x/h_n = 1.0)/R_{S_a}(T_1, h_x/h_n = 1.0)$ |
| Bearing walls | 66 | 0.898 (52.62) | 0.921 (46.51) |
| Steel Braced frames | 16 | 0.793 (61.11) | 0.845 (47.60) |
| RC walls | 41 | 0.891 (28.80) | 0.989 (39.68) |
| Masonry walls | 26 | 1.022 (27.90) | 1.027 (31.05) |
| Steel moment frames | 42 | 0.539 (71.78) | 0.564 (83.30) |
| RC moment frames | 21 | 0.557 (83.04) | 0.483 (96.80) |
| Steel dual systems | 2 | 0.466 (85.37) | 0.196 (53.83) |
| RC dual systems | 14 | 0.657 (34.99) | 0.722 (38.64) |
| All | 228 | 0.815 (54.21) | 0.787 (54.12) |

$$R_{S_a}(T, h_x/h_n) = \frac{S_a(T, h_x/h_n)}{S_a(T, h_x/h_n = 0)}$$

# Conclusions

- The $C_{px}^{(1)}$ per ASCE/SEI 7-22 Section 12.10.1 can considerably underestimate the $PFA_x$ even for ground motions with intensities lower than the design level.
- The $C_{px,6}^{(3)}$ based on ASCE/SEI 7-22 Section 12.10.3 can capture the increased $PFA_x$ caused by either the higher-mode ground spectral response accelerations or the higher-mode response contribution characteristic of the dynamic properties of the building stations.
- The factors between the ground level to the roof level of the spectral response accelerations at the second- and third-mode periods are not negligible compared with those spectral response factors at the first-mode period.
- The mean values of the spectral response factors at the second- and third-mode periods with respect to the spectral response factors at the first-mode period at roof level for steel moment frames and RC moment frames are lower than those for bearing walls, RC walls, and masonry walls. This is consistent with the formulation of the equations per ASCE/SEI 7-22 Section 12.10.3.

# Acknowledgments

The authors acknowledge the California Strong Motion Instrumentation Program (CSMIP) for their support through the project called “Validation of Seismic Design Provisions for Diaphragms and Assessment of Higher-Mode Responses on Earthquake-Resistant Buildings” and to the Chilean National Agency for Research and Development (ANID) for their support through the foreign doctoral scholarship 2020.






Any opinions, findings, and conclusions expressed in this paper are those of the authors and do not necessarily reflect the views of others acknowledged here.

18TH WORLD CONFERENCE ON EARTHQUAKE ENGINEERING
WCEE2024
MILAN

UC San Diego

# Thank you for your attention

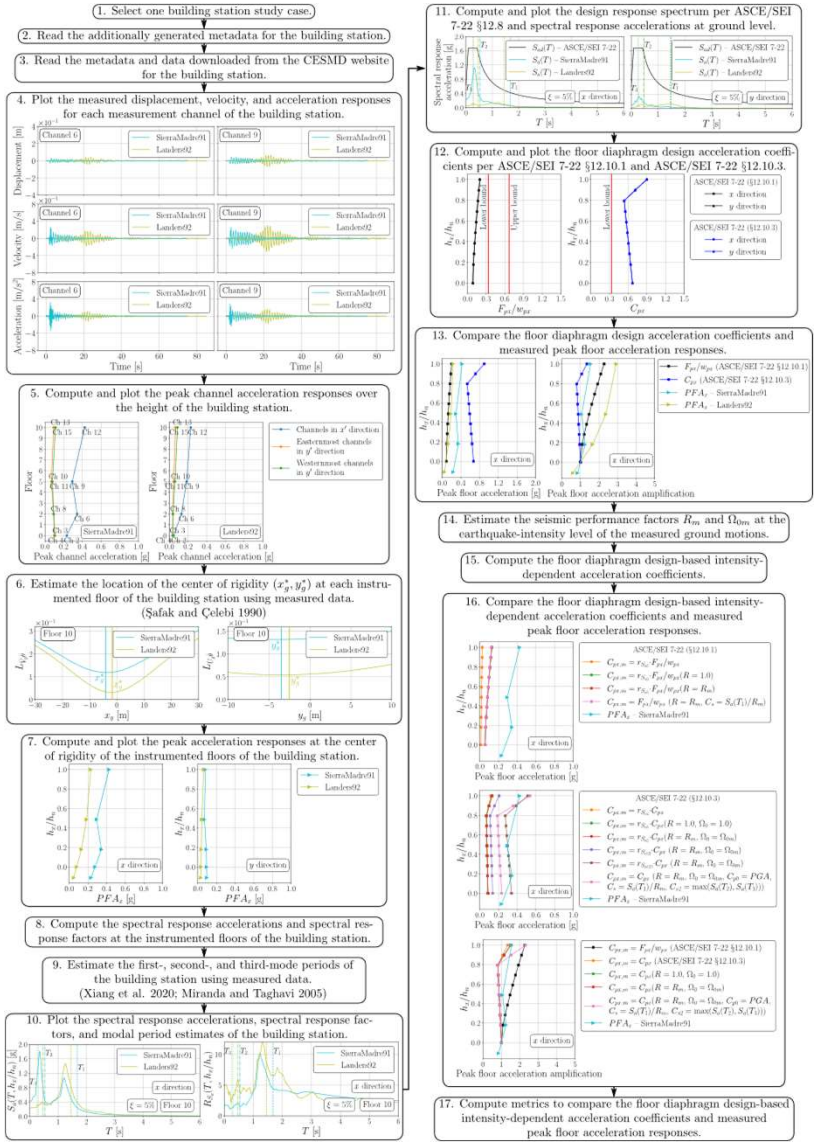
https://tsampras.ucsd.edu/

Agencia Nacional de Investigación y Desarrollo
Ministerio de Ciencia, Tecnología, Conocimiento e Innovación
Gobierno de Chile

# Data Analysis Workflow

Development of a workflow to:

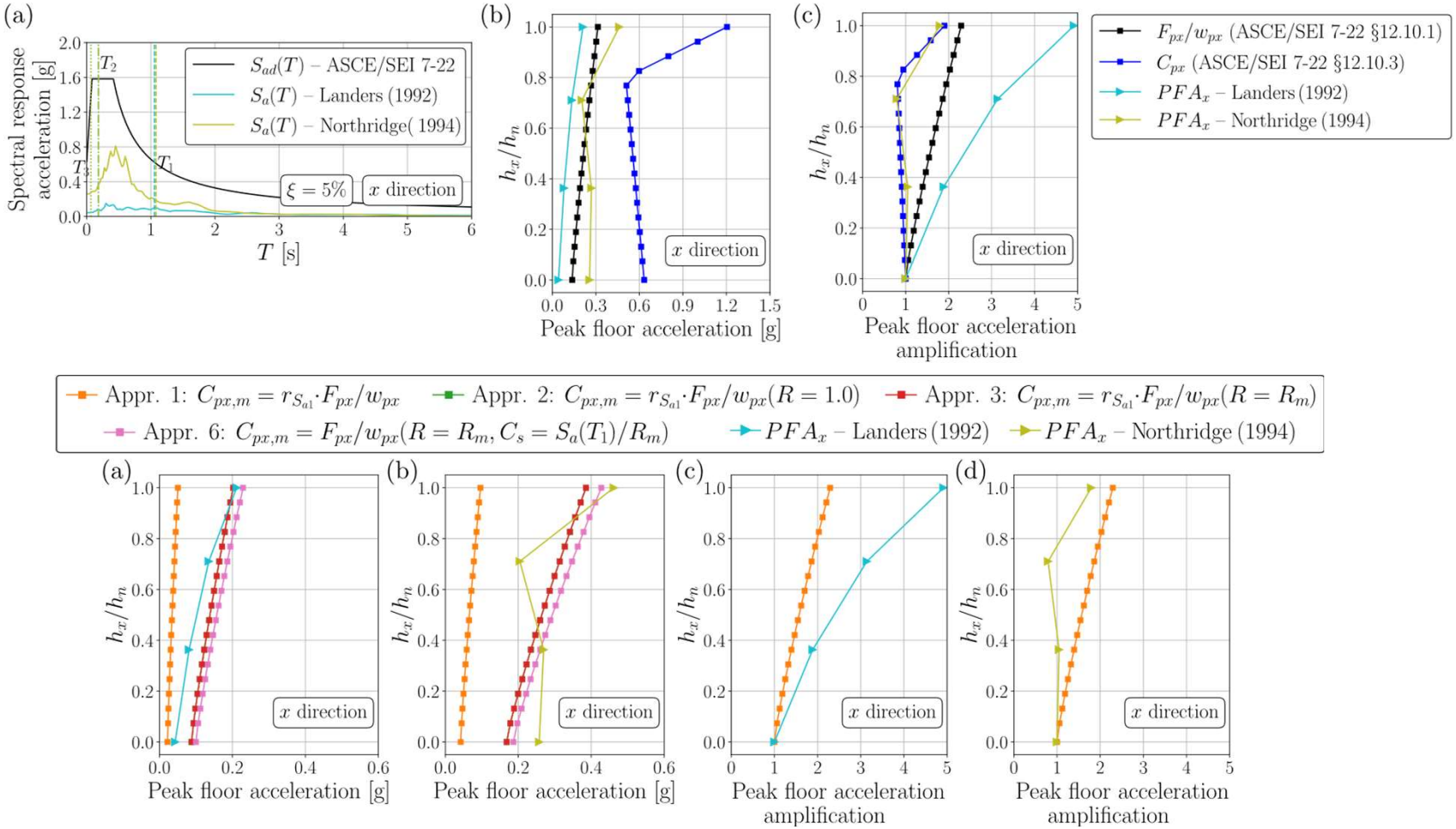
- Import, process, and plot the strong-motion data and metadata downloaded from the **CESMD website**.
- Estimate the **location of the center of rigidity**.
- Compute the **peak floor accelerations** $\boldsymbol{PFA_x}$ at the center of rigidity.
- Compute the **spectral accelerations** $\boldsymbol{S_a(T, h_x/h_n)}$ and **spectral acceleration factors** $\boldsymbol{R_{S_a}(T, h_x/h_n) = S_a(T, h_x/h_n)/ S_a(T, h_x/h_n = 0)}$ at instrumented floors.
- Estimate the **first three translational mode periods**.
- Compute the **design spectral accelerations** $\boldsymbol{S_{ad}(T, h_x/h_n)}$.
- Compute the **design acceleration coefficients** $\boldsymbol{C_{px}^{(1)}}$ and $\boldsymbol{C_{px}^{(3)}}$ per ASCE/SEI 22-7 **Sections 12.10.1 and 12.10.3**, respectively.
- Compare $\boldsymbol{PFA_x}$ with $\boldsymbol{C_{px}^{(1)}}$ and $\boldsymbol{C_{px}^{(3)}}$.




UC San Diego
JACOBS SCHOOL OF ENGINEERING
Structural Engineering

https://tsampras.ucsd.edu/

# CE24601 Building Station



# CE24601 Building Station

